arXiv:astro-ph/0011427v1 23 Nov 2000

# The Abundance and Emission of $H_2O$ and $O_2$ in Clumpy Molecular Clouds

Marco Spaans

Kapteyn Institute, P.O. Box 800, 9700 AV Groningen, The Netherlands

Ewine F. van Dishoeck

Leiden Observatory, P.O. Box 9513, 2300 RA Leiden, The Netherlands

Received _____; accepted _____

## ABSTRACT

Recent observations with the *Submillimeter Wave Astronomy Satellite* indicate abundances of gaseous $H_2O$ and $O_2$ in dense molecular clouds which are significantly lower than found in standard homogeneous chemistry models. We present here results for the thermal and chemical balance of inhomogeneous molecular clouds exposed to ultraviolet radiation in which the abundances of $H_2O$ and $O_2$ are computed for various density distributions, radiation field strengths and geometries. It is found that an inhomogeneous density distribution lowers the column densities of $H_2O$ and $O_2$ compared to the homogeneous case by more than an order of magnitude at the same $A_V$. $O_2$ is particularly sensitive to the penetrating ultraviolet radiation, more so than $H_2O$. The S 140 and $\rho$ Oph clouds are studied as relevant test cases of star-forming and quiescent regions. The SWAS results of S 140 can be accommodated naturally in a clumpy model with mean density of $2 \times 10^3$ cm$^{-3}$ and enhancement $I_{UV} = 140$ compared with the average interstellar radiation field, in agreement with observations of [C I] and $^{(13)}$CO of this cloud. Additional radiative transfer computations suggest that this diffuse $H_2O$ component is warm, $\sim 60 - 90$ K, and can account for the bulk of the $1_{10} - 1_{01}$ line emission observed by SWAS. The $\rho$ Oph model yields consistent $O_2$ abundances but too much $H_2O$, even for [C]/[O]=0.94, if $I_{UV} < 10$ respectively $< 40$ for a mean density of $10^3$ respectively $10^4$ cm$^{-3}$. It is concluded that enhanced photodissociation in clumpy regions can explain the low $H_2O$ and $O_2$ abundances and emissivities found in the large SWAS beam for extended molecular clouds, but that additional freeze-out of oxygen onto grains is needed in dense cold cores.

*subject headings*: ISM: abundances — ISM: clouds — ISM: molecules

## 1. Introduction

In contrast with the major carbon-bearing species (CO, C, $C^+$), the abundances of the major oxygen-containing atoms and molecules in general molecular clouds are still poorly understood. The best-known species is CO, which reaches large abundances of $\sim 10^{-4}$ when the shielding column of gas exceeds $A_V \approx 1$ for a typical interstellar cloud of $\sim 10^3$ cm$^{-3}$ illuminated by the average interstellar radiation field, locking up the bulk of the gas-phase carbon (e.g., Hollenbach & Tielens 1999, van Dishoeck & Black 1988). Theoretical models indicate that at the edge atomic O is abundant, but that further into the cloud, more and more of the ultraviolet radiation is attenuated so that at $A_V \approx 4$ mag, CO ceases to be the dominant oxygen-bearing species and $O_2$ reaches its peak abundance of $> 10^{-4}$, with $H_2O$ present at the level of $\sim 10^{-6}$ (e.g., Tielens & Hollenbach 1985, Lee et al. 1996). If true, then $H_2O$ and $O_2$ could be major coolants in molecular clouds (Goldsmith & Langer 1978; Neufeld, Lepp & Melnick 1995).

The launch of the *Submillimeter Wave Astronomy Satellite* (SWAS) (Melnick et al. 2000) has made it possible to look for emission lines of $H_2O$ and $O_2$ in cold molecular clouds. Although the *Infrared Space Observatory* (ISO) observed many $H_2O$ lines, it was sensitive primarily to warm, $\sim 100$ K molecular gas near young stellar objects where the $H_2O$ abundance can be enhanced due to ice evaporation and high-temperature (shock) reactions (e.g., van Dishoeck et al. 1999, Nisini et al. 2000). Measurements of, or upper limits on, the abundances of $H_2O$ and $O_2$ provide crucial tests of many aspects of the oxygen chemistry in normal molecular clouds and of the cloud structure, and hence of our theoretical understanding of such systems.

The initial SWAS results indicate that the abundances of $H_2O$ and $O_2$ in dense molecular cloud cores are surprisingly low compared with the above model predictions, about $6 \times 10^{-10} - 1 \times 10^{-8}$ for $H_2O$ and $<$ a few $\times 10^{-7}$ for $O_2$ (Ashby et al. 2000, Snell et

al. 2000a, Goldsmith et al. 2000). In contrast, ISO observations of the [O I] 63 and 145 $\mu$m lines suggest substantial abundances of atomic O in quiescent gas (e.g., Baluteau et al. 1997, Caux et al. 1999). Bergin et al. (2000) propose a model in which freeze-out of oxygen on dust grains in the form of molecular ices is significant, with the remaining oxygen in atomic form in the gas, along with CO. While freeze-out and gas-grain interactions undoubtedly play a role in dense cold clouds, we present here an alternative explanation based on clumpy molecular clouds which may be more appropriate for the general lower density molecular cloud material contained in the large SWAS beam of $3.3' \times 4.5'$. The inhomogeneous nature of molecular clouds is well established from observations of extended [C I] and [C II] (e.g., Keene et al. 1995, Stutzki et al. 1988, Plume et al. 1999), and has been modeled by various groups (e.g., Meixner & Tielens 1993, Spaans 1996, Störzer et al. 1996). It is therefore natural to also explore the $H_2O$ and $O_2$ abundances and emission in such models.

## 2. Basic Model Description

The results presented here were obtained by application of the numerical code of Spaans (1996), described further in Spaans & van Dishoeck (1997). The interested reader is referred to these papers for a description of the underlying algorithms. The code has been specifically designed to solve large chemical networks with a self-consistent treatment of the thermal balance for all heating and cooling processes known to be of importance in the interstellar medium (Spaans & Ehrenfreund 1999). The radiative transfer in the cooling lines is solved by means of a Monte Carlo approach with checks provided by an escape probability method for large line optical depths. The thermal balance includes photo-electric heating by dust grains, heating by cosmic rays, absorption of infrared photons by $H_2O$ molecules and their subsequent collisional de-excitation, and gas-grain heating. The cooling includes the coupling between gas and dust grains (Hollenbach & McKee 1989),

atomic lines of all metals, molecular lines, and all major isotopes, as described in Spaans et al. (1994) and in Neufeld et al. (1995) for the regime of very large line optical depth. All level populations are computed in statistical equilibrium at a relative accuracy of no less than $10^{-3}$, an accuracy which is also imposed on the ambient line radiation field. The combined chemical and thermal balance is required to obey a convergence criterion between successive iterations of 0.5%.

The adopted chemical network is based on the UMIST compilation (Millar, Farquhar & Willacy 1997), and is well suited for low temperature (<200 K) dense molecular clouds. A value of 0.3 is chosen for the branching ratio leading to $H_2O$ in the dissociative recombination of $H_3O^+$, with a rate coefficient of $3.3 \times 10^{-7}(T/300)^{-0.3}$ cm$^3$ s$^{-1}$. The branching ratio is consistent with the results of Vejby-Christensen et al. (1997) but higher than the value of 0.05 suggested by Williams et al. (1996). Observations and (homogeneous) models by Spaans et al. (1998) toward the translucent cloud HD 154368 favor a branching ratio of less than 0.3 (at $3\sigma$) so that the water abundance results presented here should be regarded as strict upper limits. The latest rate coefficients for important neutral-neutral reactions are adopted, in particular for $C + O_2 \rightarrow CO + O$ and $O + OH \rightarrow O_2 + H$ at $2.48 \times 10^{-12}(T/300)^{1.54}e^{-613/T}$ cm$^3$ s$^{-1}$ and $1.77 \times 10^{-11}e^{-178/T}$ cm$^3$ s$^{-1}$, respectively. The reaction of $O_2$ with neutral sulfur is not found to be a major sink for molecular oxygen. No gas-grain interactions are taken into account. The carbon and oxygen gas-phase fractions are set to $\delta_C = 0.33$ and $\delta_O = 0.35$ (C/O=0.45), but the case of $\delta_O = 0.17$ is also considered. These fractions are defined with respect to the solar values of $[C] = 4.0 \times 10^{-4}$ and $[O] = 8.3 \times 10^{-4}$. Depletions of other elements are as in Spaans & van Dishoeck (1997).

## 3. Model Results

In order to investigate the dependence of $O_2$ and $H_2O$ on density, radiation field and geometry, spherical and slab-like model clouds were computed for homogeneous and inhomogeneous density distributions (Spaans 1996). The clumpy models are defined by two parameters: the volume filling factor $f$, which fixes the fraction of the total volume that is occupied by the clumps in a two-phase density medium, and a characteristic clump size $\ell_c$, which fixes the extinction through an individual clump. The ratio between the high (h) density and low (l) density phase is chosen to be $r = 20$. It then follows that the mean total hydrogen density $n$ obeys $n = fn_{\rm h} + (1 - f)n_{\rm l}$. We model two types of regions: a star-forming cloud where the radiation field is significantly enhanced due to a nearby O or B star (e.g., S 140) and a more quiescent region such as $\rho$ Oph. For the S 140 extended molecular cloud, Spaans & van Dishoeck (1997) have constrained $f$ <50% and $\ell_c > 0.2$ pc from observations of [C I] and $^{13}$CO (Plume et al. 1994), using an average density $n \approx 10^3$ cm$^{-3}$. Recent ISO data of [C II] and [O I] confirm densities of order $10^3$ cm$^{-3}$ in the extended cloud (Li et al. 2001). We adopt here $f = 30\%$ and $\ell_c = 0.4$ pc with $n = 2 \times 10^3$ cm$^{-3}$. For models with a larger mean density the clump size $\ell_c$ is decreased by the same factor with which the mean density is increased. The enhancement of the radiation field is taken to be $I_{\rm UV}$=140 with respect to the Draine (1978) field, consistent with the enhancement at the edge of the cloud near the B0V star HD 211880. This enhancement factor decreases to $I_{\rm UV} \approx 30 - 50$ further into the extended cloud due to geometric dilution. The average interstellar radiation field incident from other directions has been included as well. The $\rho$ Oph cloud has been studied by several groups (see Liseau et al. 1999) and is modeled with $f = 20\%$ and $r = 30$, more clumpy than S 140 but with an identical value for $\ell_c$. We adopt $I_{\rm UV} \approx 10$ and $n = 10^4$ cm$^{-3}$. It thus provides an interesting comparison.

Figures 1–2 present the basic results of this work. For the inhomogeneous models the

shell/slice averaged abundances are shown for the sphere/slab as functions of $A_V$. It was found that the dispersion around the mean values by taking different cuts is not larger than about 50%, so that the systematics discussed below are robust. The following trends can be identified. First, for the same $I_{\rm UV}$ and $n$, a strong decrease in the abundances of $O_2$ and $H_2O$ is found in the inhomogeneous models, although less so for $H_2O$. The reason is that the destruction of $O_2$ remains dominated by photodissociation to large extinctions and that the clumpy structure allows ultraviolet photons to penetrate to larger depths. The effect spans a factor of 30 or more. Second, the central abundances of $H_2O$ and $O_2$ are decreased by a factor of 2-4 as the geometry is changed from a plane-parallel slab to a sphere. The reason is simply that the shielding column is larger for some rays emanating from the center of a slab compared to a sphere. A clumpy density distribution is quite effective in redistributing the directed ultraviolet radiation field from a (point-like) source into a more isotropic distribution at a depth of a few magnitudes of visual extinction (Spaans 1996). Third, a systematic trend is observed with varying dissociation parameter $U = I_{\rm UV}/n$. When this number is small, $< 5 \times 10^{-3}$, i.e., at low $I_{\rm UV}$ and/or high $n$, $H_2O$ and $O_2$ rise sharply at the edge of the cloud, and $H_2O$ quickly reaches the regime where its removal is dominated by chemistry rather than photodissociation. The total observed column of $H_2O$ and $O_2$ varies greatly with total extinction along the line of sight and it would be difficult to distinguish between homogeneous large $U$ and inhomogeneous small $U$ situations based on $H_2O$ and $O_2$ alone. Of course, large $U$ regions are bright in lines such as [C II] 158 $\mu$m, [O I] 63 and 145 $\mu$m and high-$J$ CO, whereas small $U$ regions tend to have more prominent [C I] 609 $\mu$m emission, in particular when they are clumpy.

## 4. Discussion and Comparison with Observations

### 4.1. $H_2O$ and $O_2$ abundances

The observational results represent abundances integrated over depth. Thus, mass-weighted abundances for the spherical models have been computed for comparison with observations. Specifically, the mean abundance $X(r)$ enclosed within some fractional radius $r$ is given by integration of the abundance $A(r)$ through $X(r)=\int_0^r A(r')r'^2dr'/\int_0^r r'^2dr'$, where 0 is at the center and 1 at the edge of the model cloud. Note that only 1/8 of the mass is contained inside the half radius of the spherical constant density model cloud, while this would be 1/2 for a $1/r^2$ density profile.

For the clumpy, spherical model of Figure 1 (top and middle) the above approach leads to a predicted mean $H_2O$ abundance $X(1) = 3 \times 10^{-8}$ and an $O_2$ abundance of $4 \times 10^{-10}$ for a typical total depth of $A_V = 10$ mag. Snell et al. (2000a) detected $H_2O$ emission from the S 140 dense star-forming core and PDR region with SWAS, but not from the surrounding extended molecular cloud. Their inferred abundances of $\sim 10^{-8}$ (see also the detailed analysis by Ashby et al. 2000) for the core and $< 10^{-8}$ for the extended cloud are only a factor of three lower than our model results and consistent within the factor of three or more uncertainty in their assumed density (the inferred $H_2O$ abundance scales with the inverse of density). Figure 1c (bottom) shows the effect of increasing the density to $5 \times 10^4$ cm$^{-3}$ for the S 140 environment. The smaller value of $U$ causes photodissociation to play a lesser role in the removal of $O_2$ and $H_2O$, and hence clumpiness is of less importance. The model (mass weighted) abundances are $3 \times 10^{-7}$ and $4 \times 10^{-8}$ for $H_2O$ and $O_2$, respectively.

The model for $\rho$ Oph appears less successful in reproducing the observed abundances of $O_2$ and $H_2O$. The mass weighted $H_2O$ abundance for Figure 2c (bottom) is $3 \times 10^{-7}$, a factor of $\sim$100 above the measured value. Panels 2a and b (top and middle), which are representative of larger values of $U$ and roughly consistent with the results of Liseau et al. (1999) who found $n_{\rm H} = 3 \times 10^3 - 3 \times 10^4$ cm$^{-3}$, yield mass-weighted $H_2O$ abundances of

$5 \times 10^{-8}$ and $2 \times 10^{-8}$, respectively. From the discussion in §3, it follows that the S 140 case yields better agreement with the observations mainly because of its larger illumination (and $U$ parameter). The clumpy models enhance the importance of photodissociation of $H_2O$ and $O_2$ deeper into the cloud, and therefore work best for a strong incident radiation field.

In all inhomogeneous models with $n \approx 10^3$ cm$^{-3}$, the mass weighted abundance of $O_2$ is below $10^{-7}$, both for S 140 and $\rho$ Oph, consistent with the overall SWAS upper limits as well as the specific upper bounds for S 140, $< 7 \times 10^{-7}$, and $\rho$ Oph, $< 3 \times 10^{-7}$ (Goldsmith et al. 2000). Only the quiescent model of Figure 2c (bottom) with high density and low $I_{\rm UV}$, yields a mass weighted $O_2$ abundance of $10^{-6}$. This is a factor of a few above the observational limit (Goldsmith et al. 2000), but this is easily alleviated by a modest increase in the [C]/[O] ratio (Bergin et al. 2000). To test the latter possibility, we have run a model with an oxygen depletion of 0.17 and [C]/[O]=0.94. A decrease in the mass weighted $H_2O$ ($O_2$) abundance of a factor of 5 (20) is found, bringing the model in agreement with the observations for S 140 and factors of 20, 4 and 2 too high for $H_2O$ toward $\rho$ Oph in models 2a, b and c, respectively, although a smaller value for the $H_3O^+$ branching ratio of 0.05 instead of 0.3 could further reduce these discrepancies.

### 4.2. $H_2O$ and $O_2$ emission

In order to verify whether the low abundances of $H_2O$ and $O_2$ found for the clumpy model clouds can also reproduce the bulk of the observed emission, radiative transfer computations have been performed using a Monte Carlo method (Spaans 1996). It was found that two effects dominate the emissivity of the $H_2O$ $1_{10} - 1_{01}$ line: temperature and geometry. The temperature is very important because it influences both the ortho-para ratio of the main collision partner $H_2$, 0.1 at 30 K and 1.0 at 80 K (Neufeld & Sternberg 1999), as well as the collisional excitation rate. The $H_2$ ortho-para ratio is a crucial parameter

to compute rigorously from the thermal balance and FUV pumping since the o-$H_2$ $J$=1 collision rates with $H_2O$ are more than an order of magnitude larger than the p-$H_2$ $J$=0 rates (Phillips, Maluendes & Green 1996). The geometry is important because the $1_{10} - 1_{01}$ line is optically thick but effectively thin. This implies that line photons emitted by the warm edges of a spherical clump can interact with water molecules in the colder interior, and so constitute an excitation term that raises the level population in the $1_{10}$ state. Note in this that the curvature of the sphere causes the warm gas to cover $4\pi$ steridians, unlike the slab case. It is found that a spherical geometry, for the S 140 temperature profile given below, raises the $1_{10} - 1_{01}$ line strength with a factor of 2.4 compared to that from the plane-parallel slab. Furthermore, for identical physical conditions, a plane-parallel slab model yields a temperature profile that is systematically 20-30% cooler than for the corresponding spherical case, mainly because the latter possesses more lower extinction lines of sight.

The thermal balance yields a temperature of 150 (80) K at the edge of S 140 ($\rho$ Oph) and 20 (10) K at its center. The mass weighted $H_2O$ temperatures are $\sim$ 80 K and $\sim$ 30 K for S 140 and $\rho$ Oph, respectively. For S 140, these values refer to the model of Fig. 1$a/b$, and for $\rho$ Oph to the model of Fig. 2$b$. The S 140 value is significantly larger than the typical temperature in dense cores, $\sim$ 30 K. The resulting integrated line intensities convolved with the SWAS beam are 1.6 K km s$^{-1}$ and 3.8 K km s$^{-1}$ for S 140 and $\rho$ Oph, respectively. The clumpy S 140 model can thus reproduce the observed value (1.7 K km s$^{-1}$) quite nicely, but the clumpy $\rho$ Oph $H_2O$ emission, just as the abundance, is too large compared to the observed value of 0.8 K km s$^{-1}$. Use of a plane-parallel geometry would reduce the discrepancy for $\rho$ Oph significantly. In both instances, the bulk of the signal in the SWAS beam is associated with the PDR. In fact, *the $H_2O$ emission arises mainly from the warm, $\sim$60-90 K, edges of irradiated clumps*. Therefore, a strong correlation should exist between the SWAS $H_2O$ emission and high$-J$ (e.g. 5-4, 6-5) CO emission. Such a correlation is in

fact observed toward M 17SW (Snell et al. 2000b). It is the elevated temperatures at the surfaces of the clumps that makes the results so sensitive to the ortho-para ratio. For the case of S 140, the extended molecular cloud gives an emission that is a factor of 30 weaker at a position $4'$ north-east of the PDR, due to the lower ambient temperature, consistent with observations. The $O_2$ $N_J = 3_3 - 1_2$ line is truly optically thin and yields, due to its simpler excitation, more robust results. We find $1.8 \times 10^{-5}$ K km s$^{-1}$ and $2.3 \times 10^{-3}$ K km s$^{-1}$ for the S 140 and $\rho$ Oph case, respectively.

ISO $H_2O$ observations suggest that much of $H_2O$ toward star-forming cores such as S 140 is associated with a small region with enhanced $H_2O$ surrounding the young stellar object(s) (e.g., Wright et al. 1997, Ceccarelli et al. 1999). Since this emission is subsequently beam-diluted in the large SWAS beam, its contribution could be small and still be consistent with the fact that the lower density gas in the SWAS beam is capable of reproducing the bulk of the detected water emission by SWAS. We have verified this by adding a clumpy star-forming core with $n = 10^4$ cm$^{-3}$ and a size of $\sim 0.5$ pc (Zhou et al. 1994), and the same values for $f$ and $r$, to the S 140 extended molecular cloud as in Spaans & van Dishoeck (1997). Even though the mean water abundance goes up by a factor of 30, the lower kinetic temperature and smaller spatial extent yield a relative contribution of $\sim 20\%$ after convolution with the SWAS beam. Furthermore, the Zhou et al. CS observations can be well reproduced by this clumpy core that includes densities of up to $\sim 10^5$ cm$^{-3}$ and temperatures that are still $\sim 30 - 40$ K. [1]

Bergin et al. (2000) have argued against the importance of photodissociation because

[1]At even higher densities ($\sim 10^7$ cm$^{-3}$) and smaller scales ($\sim 200 - 400$ AU), the $H_2O$ abundance becomes even larger and the region emits thermally at about 100 K. Strong beam-dilution limits this contribution to the SWAS signal to less than 2% at the distance of $\sim 910$ pc for S 140.

it would affect the abundances of other species such as $NH_3$ as well. The S 140 model, including the star-forming core as above, was checked for consistency with the observational $NH_3$ values of $2 - 9 \times 10^{14}$ cm$^{-2}$ (Ungerechts, Winnewisser & Walmsley 1986). Our model value of $\sim 4 \times 10^{14}$ cm$^{-2}$ is not in conflict with observations. In addition, even a moderate enhancement in $NH_3$ formation due to grain-surface chemistry is likely to resolve any mild discrepancy. For the extended molecular cloud outside the core there are no observational constraints for ammonia. Future observational and theoretical studies should investigate other species whose abundances are sensitive to photodissociation, such as the CN/HCN and $C_2H/HCO^+$ ratios (e.g., Jansen et al. 1995). This work has not addressed the effects of time-dependent chemistry and freeze-out on the $O_2$ and $H_2O$ abundances (Bergin et al. 2000, Viti 2000, private communication). Our results suggest that clumpiness is a viable alternative explanation for extended lower-density molecular clouds in star-forming regions like S 140 with high radiation field, but they also strengthen the case for time-dependent chemistry and freeze-out for a more quiescent dense region like $\rho$ Oph. The freeze-out models may in fact benefit from adoption of a clumpy structure since the central dust temperature is enhanced by the higher internal ultraviolet field, thus providing a mechanism to moderate the very rapid freeze-out. Future observatories such as ODIN and the HIFI instrument on the *Far Infrared and Submillimeter Telescope* (FIRST) will have increased sensitivity, and, in the case of FIRST, a much smaller beam. Therefore, more definite tests of the various classes of models will be forthcoming in this decennium.

We are grateful to Ted Bergin, Gary Melnick, Matt Ashby and Serena Viti for stimulating discussions regarding the SWAS results, to Steven Doty for assistance with the chemistry, and to the referee, Ted Bergin, for his constructive comments that helped to improve this paper.

## REFERENCES

Ashby, M.L.N., Bergin, E.A., Plume, R., et al., 2000, ApJ, 539, L119

Baluteau, J.-P., Cox, P., Cernicharo, J., et al., 1997, A&A, 322, L33

Bergin, E.A., Melnick, G.J., Stauffer, J.R., 2000, 539, L129

Caux, E., Ceccarelli, C., Castets, A., et al., 1999, A&A, 347, L1

Ceccarelli, C., Caux, E., Loinard, L., Castets, A., Tielens, A.G.G.M., Molinari, S., Liseau, R., Saraceno, P., Smith, H. & White, G., 1999, A&A, 342, L21

Draine, B.T., 1978, ApJS, 36, 595

Goldsmith, P.F., Melnick, G.J., Bergin, E.A., et al., 2000, ApJ, 539, L123

Hollenbach, D.A. & Tielens, A.G.G.M. 1999, Rev. Modern Phys., 71, 173

Hollenbach, D.A. & McKee, C.F., 1989, ApJ, 342, 306

Jansen, D.J., van Dishoeck, E.F., Black, J.H., Spaans, M. & Sosin, C., 1995, A&A, 302, 223

Keene, J., Blake, G.A., Phillips, T.G., Huggins, P.J. & Beichman, C.A., 1985, ApJ, 299, 967

Lee, H.-H., Herbst, E., Pineau des Fôrets, G., Roueff, E. & le Bourlot, J., 1996, A&A, 311, 690

Li, W., et al., 2001, in preperation

Liseau, R., White, G.J., Larsson, B., Sidher, S., Olofsson, G., Kaas, A., Nordh, L., Caux, E., Lorenzetti, D., Molinari, Nisini, B. & Sibille, F., 1999, A&A, 344, 342

Meixner, M.M. & Tielens, A.G.G.M., 1993, ApJ, 405, 216

Melnick, G.J., Ashby, M.L.N., Plume, R., et al., 2000, ApJ, 539, L87

Millar, T.J., Farquhar, P.R.A. & Willacy, K., 1997, A&AS, 121, 139

Neufeld, D.A. & Sternberg, A., 1999, ApJ, 516, 371

Neufeld, D.A., Lepp, S. & Melnick, G.J. 1995, ApJS, 100, 132

Nisini, B., Benedettini, M., Giannini, T., et al., 2000, A&A, 360, 297

Phillips, T.R., Maluendes, S. & Green, S., 1996, ApJS, 107, 467

Plume, R., Jaffe, D.T., Tatematsu, K., Evans, N.J.II, Keene, J., 1999, ApJ, 512, 768

Plume, R., Jaffe, D.T. & Keene, J., 1994, ApJL, 425, L49 Chem. Phys. Lett., 269, 88

Snell, R.L., Howe, J.E., Ashby, M.L.N., et al., 2000a, ApJ, 539, L101

Snell, R.L., Howe, J.E., Ashby, M.L.N., et al., 2000b, ApJ, 539, L97

Spaans, M. 1996, A&A, 307, 271

Spaans, M. & van Dishoeck, E.F. 1997, A&A, 323, 953

Spaans, M., Tielens, A.G.G.M., van Dishoeck, E.F. & Bakes, E.L.O., 1994, ApJ, 437, 270

Spaans, M. & van Langevelde, H.J. 1992, MNRAS, 258, 159

Störzer, H., Stutzki, J. & Sternberg, A., 1996, A&A, 310, 592

Stutzki, J., Stacey, G.J., Genzel, R., Harris, A.I., Jaffe, D.T., Lugten, J.B., 1988, ApJ, 332, 379

Takahashi, T., Hollenbach, D.J. & Silk, J. 1983, ApJ, 275, 145

Tielens, A.G.G.M. & Hollenbach, D.A. 1985, ApJ, 291, 722

van Dishoeck, E.F., ed. "Molecules in Astrophysics: Probes and Processes", 1997, IAU Symp. 178, Kluwer

van Dishoeck, E.F. & Black, J.H., 1988, ApJ, 334, 771

van Dishoeck, E.F., Black, J.H., Boogert, A.C.A., et al., 1999, ESASP, 427, 437

Vejby-Christensen, L., Andersen, L.H., Heber, O., Kella, D., Pedersen, H.B., Schmidt, H.T. & Zajfman, D., 1997, ApJ, 483, 531

Williams, T.L., Adams, N.G., Babcock, L., Herd, C.R. & Geoghegan, M., 1996, MNRAS, 282, 413

Wright, C.M., van Dishoeck, E.F., Helmich, F.P., Lahuis, F., Boogert, A.C.A., & de Graauw, Th. 1997, in First ISO workshop on analytical spectroscopy, ESA SP-419 (Noordwijk: ESTEC), p. 37

Zhou, S., Butner, H.M., Evans, N.J. II, Guesten, R., Kutner, M.L. & Mundy, L.G., 1994, ApJ, 428, 219

This manuscript was prepared with the AAS LaTeX macros v4.0.

Fig. 1.— Models appropriate of the S 140 extended molecular cloud. 1a (top): Model cloud with $n = 2 \times 10^3$ cm$^{-3}$ and $I_{\rm UV} = 140$. Solid lines are clumpy spherical model, dashed lines homogeneous spherical model; 1b (middle): Model cloud with $n = 2 \times 10^3$ cm$^{-3}$ and $I_{\rm UV} = 140$. Solid lines are clumpy spherical model, dashed lines clumpy slab model; 1c (bottom): Model cloud with $n = 5 \times 10^4$ cm$^{-3}$ and $I_{\rm UV} = 140$. Solid lines are clumpy spherical model, dashed lines homogeneous slab model.

Fig. 2.— Models appropriate for the $\rho$ Oph cloud. 2a (top): cloud with $n = 10^3$ cm$^{-3}$ and $I_{\rm UV} = 10$. Solid lines are clumpy spherical model, dashed lines homogeneous slab model; 2b (middle): Model cloud with $n = 10^4$ cm$^{-3}$ and $I_{\rm UV} = 40$. Solid lines are clumpy spherical model, dashed lines homogeneous spherical model; 2c (bottom): Model cloud with $n = 10^4$ cm$^{-3}$ and $I_{\rm UV} = 10$. Solid lines are clumpy spherical model, dashed lines homogeneous spherical model.

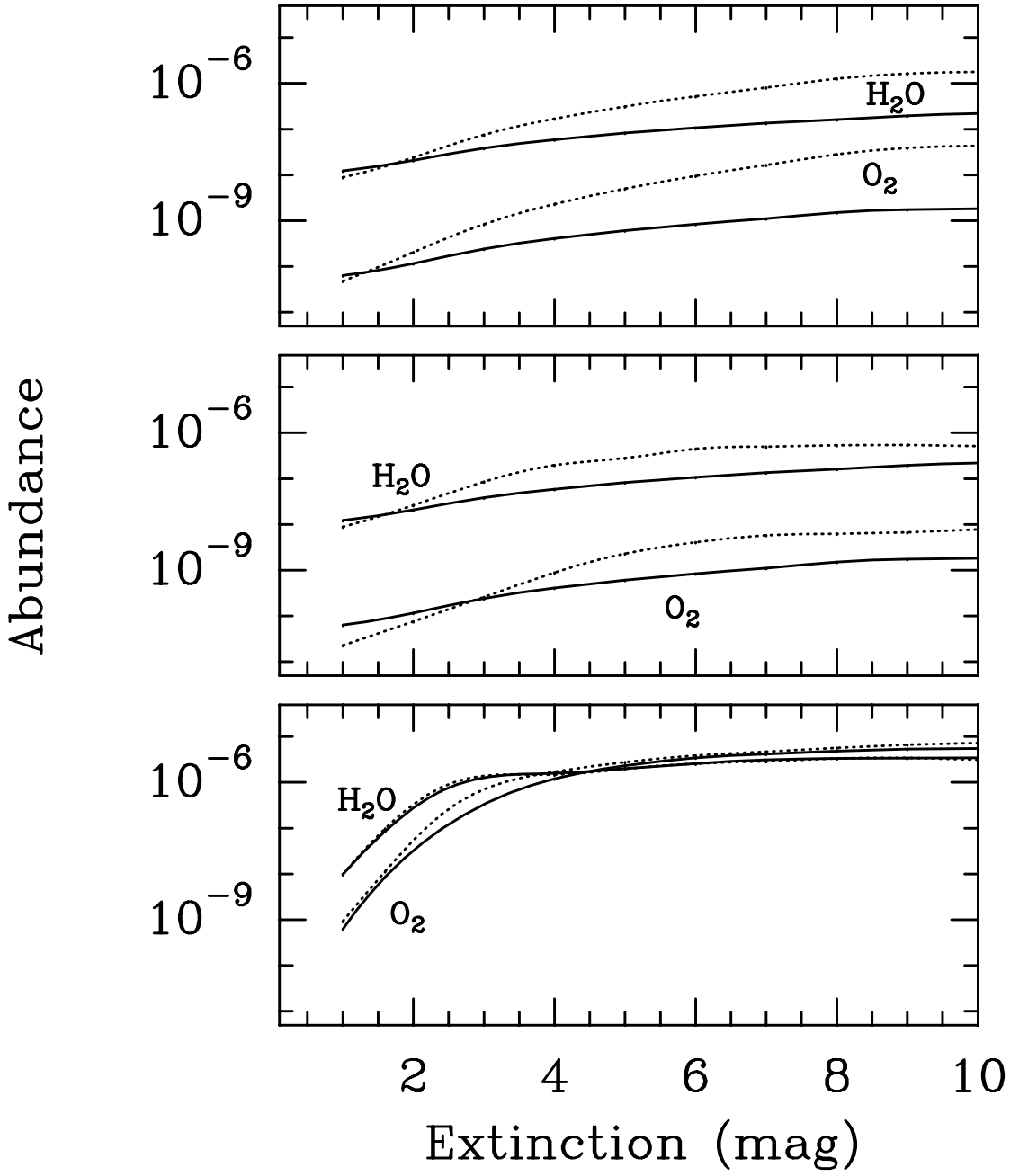
Abundance
$10^{-6}$
$10^{-9}$
$H_2O$
$O_2$
$10^{-6}$
$10^{-9}$
$H_2O$
$O_2$
$10^{-6}$
$10^{-9}$
$H_2O$
$O_2$
2
4
6
8
10
Extinction (mag)

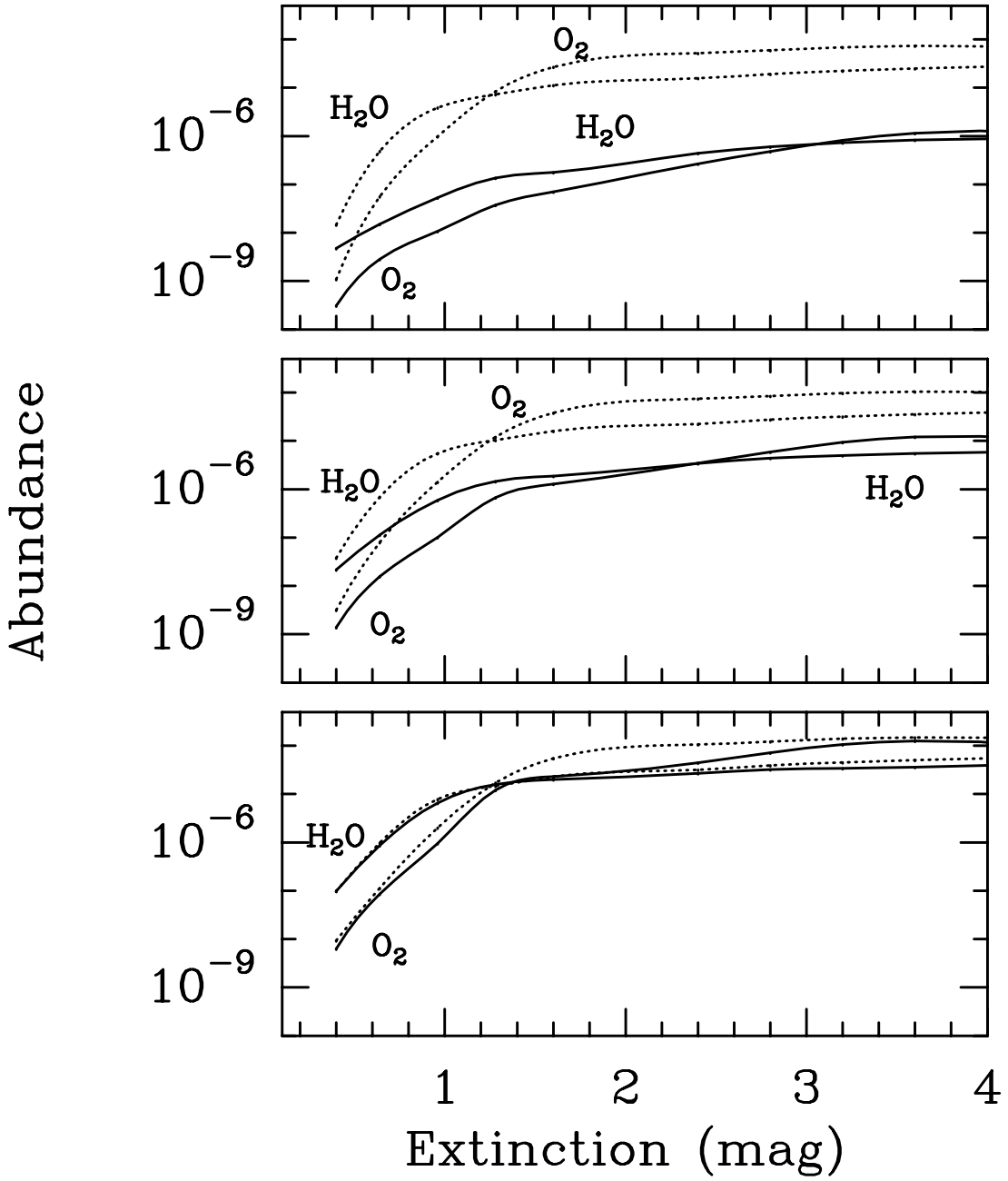
Abundance
$10^{-6}$
$10^{-9}$
$H_2O$
$O_2$
1
2
3
4
Extinction (mag)